Hindawi Publishing Corporation
Journal of Nanomaterials
Volume 2015, Article ID 451405, 9 pages
http://dx.doi.org/10.1155/2015/451405

Research Article

Lipoamino Acid Coated Superparamagnetic Iron Oxide Nanoparticles Concentration and Time Dependently Enhanced Growth of Human Hepatocarcinoma Cell Line (Hep-G2)

Ahmad Gholami,[1,2] Sara Rasoul-amini,[3] Alireza Ebrahiminezhad,[2,4] Seyed Hassan Seradj,[5] and Younes Ghasemi[1,2]

[1]*Department of Pharmaceutical Biotechnology, School of Pharmacy, Shiraz University of Medical Sciences, P.O. Box 71345-1583, Shiraz, Iran*
[2]*Pharmaceutical Sciences Research Center, Shiraz University of Medical Sciences, P.O. Box 71345-1583, Shiraz, Iran*
[3]*Department of Medicinal Chemistry, School of Pharmacy, Shiraz University of Medical Sciences, P.O. Box 71345-1583, Shiraz, Iran*
[4]*Department of Medical Biotechnology, Fasa University of Medical Sciences, Fasa 74616-86688, Iran*
[5]*Department of Pharmacognosy, School of Pharmacy, Shiraz University of Medical Sciences, P.O. Box 71345-1583, Shiraz, Iran*

Correspondence should be addressed to Younes Ghasemi; ghasemiy@sums.ac.ir

Received 17 November 2014; Revised 14 March 2015; Accepted 23 March 2015

Academic Editor: Paulo Cesar Morais

Superparamagnetic iron oxide nanoparticles (SPION) have been widely used in medicine for magnetic resonance imaging, hyperthermia, and drug delivery applications. The effect of SPION on animal cells has been a controversial issue on which there are many contradictions. This study focused on preparation of SPION with novel biocompatible coatings, their characterization, and cytotoxicity evaluation. An amino acid (glycine) and two novel lipo-amino acids (2 amino-hexanoic acid and 2 amino-hexadecanoic acid) coated magnetic nanoparticles were characterized by various physicochemical means such as X-ray diffraction (XRD), transmission electron microscopy (TEM), vibrating sample magnetometry (VSM), differential scanning calorimetry (DSC), and infrared spectroscopy (FT-IR). The cytotoxicity profile of the synthesized nanoparticles on Hep-G2 cells as measured by MTT assay showed the nanoparticles are nontoxic and the cell growth is promoted by SPION. Moreover, lipoamino acid coating SPION appear more beneficial than the other ones. By increasing concentration of SPION, growth enhancing impact will attenuate and toxicity will appear. Although the aggregation of SPION can affect the results, the gradual delivery of ferric/ferrous ions into cells is the main cause of this growth promotion effect. Conclusively, this study shows that lipoamino acid coating SPION can be used for various biomedical purposes.

1. Introduction

The only FDA approved metal oxide nanoparticles are superparamagnetic iron oxide nanoparticles (SPION) that hold great potential in a vast variety of medical applications including diagnostic magnetic resonance imaging (MRI), intracellular labeling, tissue engineering, DNA detection, magnetic transfections, targeted drug delivery, and targeted antiproliferative hyperthermia therapy [1, 2]. Despite considerable potential benefits, exposure of cells to SPION may be associated with significant undesirable side effects. To date, the available researches about effects of magnetic nanoparticles on a variety of animal cell lines have been controversial and sometimes even contradictory. Many previous studies revealed that SPION can interrupt the integrity of cell membrane and adversely affect normal cell functionalities [3]. The SPION elicit massive cellular internalization associated with major depletion of microfilaments and interference with actin distribution in cells, leading to spherical shape cells with smaller sizes [4]. They promote lipid and protein peroxidation, nucleic acid damage, and necrosis [5]. The surface coating by biocompatible substances such as dextran, polyvinyl

alcohol, polyethylene glycol, pullulan, dimercaptosuccinic acid, and polypeptides can greatly alleviate and in most cases completely eliminate these large adverse effects of SPION. Appropriate surface coating of the magnetic nanoparticles also may protect them against agglomeration, limit their nonspecific cell interactions, and tune pharmacokinetics and endosomal release. In addition, surface functionalization has become an integral part of SPION designs to allow for addition of various biomolecules for diagnostic and therapeutic purposes [6]. However, some studies showed that SPION at certain concentration have no apparent toxic impact and even show beneficial effect on some animal cell lines [7–9]. It seems that the effect of both uncoated and naked SPION on the growth of cell cultures depends on type of the cell line. Wu et al. [10] demonstrated that SPION induce a dose dependent cytotoxicity in human umbilical vein endothelial cells. Mahmoudi et al. [11] reported toxicity in mouse fibroblast cell line L929 induced by naked SPION, while the coated ones had lower toxicity. In spite of some exceptions, generally the articles stated that naked SPION have great toxic impact on cell lines, while SPION with a certain biocompatible coating not only did not show cell toxicity but also in some cases induced cell proliferation [12, 13]. The possible explanation of this phenomenon might be the different cell membrane interactions with the nanoparticles [12] or due to difference in uptake through cell endocytosis [14]. Various factors such as surface electrostatic charge, surface coatings, particle size, degree of agglomeration, and type of tested cell line play a role in endocytosis and the resultant cytotoxicity of SPION [15].

There are only a few reports about effects of SPION on human hepatocarcinoma cell line, Hep-G2. A preliminary study showed that SPION at low doses have beneficial effect as evidence by cell proliferation in this cell line for 24 and 48 hours of exposure [16]. In our recent study, we found that SPION promote the growth of Hep-G2 cell line and biocompatible coatings, L-lysine and 3-aminopropyltriethoxysilane, can increase these biological benefits [17].

Lipoamino acids (LAAs) have become more attractive due to their chemical simplicity and versatility, surface activity, extensive biological activity, and low toxicity profile [18]. They play an important role in conjugation with a wide variety of functional groups of therapeutic agents to increase their hydrophobicity [19], *in vitro* cellular penetration, and *in vivo* oral absorption [20]. Toxicity levels of Hep-G2 cells and their changes in the cell cultures due to SPION exposure were determined using the MTT assay because of well integrity and comparison of results with previous studies.

The present work was designed to study the potential cell toxicity of some novel lipoamino acid coated SPION compared with glycine coated and naked SPION on Hep-G2 cell lines. To this end, we will synthesize magnetic Fe_3O_4 nanoparticles and functionalize with two different LAA and glycine. Also, we will focus on LAAs, resembling alkylated amino acids, as a novel coating for SPION to improve physicochemical characteristics of nanoparticles and facilitate their penetration across the biological barrier.

2. Materials and Methods

2.1. Synthesis of Lipoamino Acid. Lipoamino acid synthesis was carried out according to Gibbons et al. [21]. Briefly, 110 mmol of diethyl acetamidomalonate was dissolved in 85 mL solution of sodium and ethanol (3% W/V) and refluxed with 150 mmol appropriated alkyl bromide overnight at 70°C. Then, 180 mL HCl (1 M) and 20 mL dimethylformamide were added to the obtained precipitate and were refluxed for another overnight. After cooling, 900 mL ammonium hydroxide 32% was added to reach pH 7-8. The filtered precipitate was washed three times with absolute ethanol. 1-Bromomethane and 1-bromotetradecane were used to synthesize 2-amino-hexanoic acid (LAA4) and 2-amino-hexadecanoic acid (LAA14), respectively.

2.2. Synthesis of Naked SPION. Naked SPION were synthesized by coprecipitation of ferric chloride and ferrous sulfate salts with ammonium hydroxide under inert atmosphere. In brief, $FeSO_4{\cdot}4H_2O$ (0.6 g, 2.2 mmol) and $FeCl_3{\cdot}6H_2O$ (1.17 g, 3.8 mmol) were dissolved in 50 mL degassed ddH_2O and the solution was stirred at 70°C under a nitrogen atmosphere. After 60 min, 5 mL ammonium hydroxide solution (32%) was quickly added until the target pH (11) was reached. The solution was stirred for another 60 min. Black precipitate was separated by a permanent magnet, washed by degassed ddH_2O five times, and dried overnight in oven at 50°C. All the remaining nanoparticles were kept under nitrogen at 4°C until any further work was carried out.

2.3. Synthesis of Surface Functionalized SPION. Surface functionalized SPION were also synthesized in one step by aqueous coprecipitation method, using salts of ferric chloride and ferrous sulfate and a lipoamino acid (LAA4 or LAA14) or glycine that were dissolved in degassed ddH_2O in the molar ratio of 2 : 1 : 4. After 90 min agitation at 70°C under inert (N_2) atmosphere, 5 mL ammonium hydroxide (32%) was rapidly injected until pH 11 was reached and the reaction was continued for 60 min. The burnt brown-colored precipitate was separated under magnetic field and washed five times by degassed ddH_2O and then dried overnight in oven at 50°C. LAA4 coated SPION (L4@Fe_3O_4), LAA14 coated SPION (L14@Fe_3O_4), and glycine coated SPION (Gly@Fe_3O_4) were separately kept in glass vials under nitrogen at 4°C until cytotoxicity assays were done.

2.4. Characterization of LAA and SPION. For nanoparticles, X-ray powder diffraction (XRD) measurements were done with a Siemens D5000 diffractometer, using Cu-Ka radiation. Transmission electron microscopy (TEM) investigations have been done using a Philips, CM 10, HT 100 kV transmission electron microscope. Magnetic properties of nanoparticles were measured by Meghnatis Daghigh Kavir Co., using vibrating sample magnetometer (VSM) technique. Differential scanning calorimetry (DSC) was performed by a BAHR Thermoanalyser DSC 302 apparatus using Al_2O_3 as standard. Synthesized LAA and all nanoparticles were also

characterized by Fourier Transformed Infrared spectroscopy (FTIR, Bruker, Vertex 70, FT-IR Spectrometer).

2.5. In Vitro Cell Toxicity Assay. Cytotoxicity of the naked and surface functionalized SPION on Hep-G2 cell line was evaluated using standard MTT colorimetric assay. Seven concentrations of nanoparticles from 1 to 500 μg/mL were selected. Hep-G2 cell pellets were suspended in RPMI 1640 media containing 10% fetal bovine serum with a concentration of 1×10^5 cells/mL. Then 100 μL of suspension was seeded in 96-well plates to obtain 1×10^4 cells/well and incubated in a humidified atmosphere of 5% CO_2 and 95% air at 37°C to allow the cells to adhere and reach roughly 80% confluence. After 24 h, culture prepared by media in each well was replaced by 100 μL of each sample suspension which was previously prepared by RPMI media and the plates incubated at 37°C in atmosphere of 5% CO_2 and 95% air. After 24 or 48 h, the medium was removed and the wells were washed twice for 3 min with 100 μL phosphate buffer saline (PBS). A total of 25 μL MTT [3-(4,5-dimethylthiazol-2-yl)-2,5-diphenyltetrazolium bromide] solution (4 mg/mL in media) was added to each well and incubated again for 3 h at 37°C. The reaction was stopped and the formazan dye was solubilized by adding 100 μL of dimethyl sulfoxide (DMSO). To completely dissolve formazan crystals, plate was shaken well and the optical absorption of solution was read at 540 nm using a microplate spectrophotometer (PowerWave X52, BioTek Instruments Inc., US). The average value was calculated from six treated wells and values for medium alone were subtracted. In this experiment, the wells containing culture medium were regarded as negative control (0% viability) and wells containing untreated HepG2 cells were considered as positive control (100%). The optical density values (OD) of all samples were then analyzed by

$$\% \text{ cell viability} = \frac{[\text{OD (Cells + SPION)} - \text{OD (SPION)}]}{[\text{OD (Cells)} - \text{OD (RPMI)}]} \times 100. \quad (1)$$

The cell viability of six wells containing the same sample was compared with positive control.

2.6. Statistical Analysis. All statistical analyses were performed using GraphPad prism v5.0.4.533 (GraphPad Software, San Diego, CA, USA). For statistical comparison of cytotoxic activity, the analysis of variance combined with Tukey's multiple range test was performed. This experiment was repeated six times. A P value below 0.05 was considered as statistically significant.

3. Results and Discussions

3.1. X-Ray Diffraction Analysis. XRD is usually performed to characterize the crystallinity of particles and is sometimes used for identification of the average diameter of the nanoparticles. Figure 1 indicates XRD patterns of the naked and surface modified SPION. The peaks of the synthesized

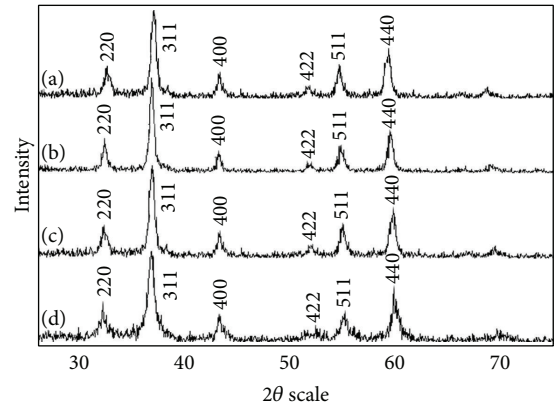

Figure 1: XRD patterns of naked SPION (a) and surface modified SPION: L14@Fe_3O_4 (b), L4@Fe_3O_4 (c), and Gly@Fe_3O_4 (d).

nanoparticles are compared with those of the standard data for magnetite and confirmed the formation of Fe_3O_4. A series of characteristic peaks at 2θ equal to 30°, 35°, 43°, 53°, 57°, and 63°, which corresponds to (220), (311), (400), (422), (511), and (440) Bragg reflection, respectively, in agreement with standard magnetite (Fe_3O_4) XRD patterns [22], identify that all SPION have cubic spinel structure [22, 23]. The result also shows that the surface modification did not change the crystalline structure of the SPION.

3.2. Morphology and Particle Size Analysis. Figure 2 displays TEM micrographs of SPION and its modified forms. As shown in the figure, in addition to the dispersed and well-separated features, the prepared colloids also exhibited some degree of aggregated morphology. The size distribution was determined by measuring diameters of more than one hundred NPs randomly selected on the TEM micrographs. The naked SPION L14@Fe_3O_4, L4@Fe_3O_4, and Gly@Fe_3O_4 nanoparticles were almost monodisperse and most of them were approximately spherical with the mean sizes of 11 ± 3, 7 ± 2, 9 ± 2, and 9 ± 4 nm, respectively. Synthesis of nanoparticles in presence of amino or lipoamino acids provided nanoparticles with slightly smaller size (3–11 nm) compared to naked nanoparticles (9–16 nm).

Biological studies showed that nanoparticles size has a considerable effect on the toxicity of SPION [24]. As presence of amino acid like-chemical materials may have inhibitory effect on size of nanoparticles during synthesis process of SPION [25], the reaction time of surface coated SPION has been increased to 90 min compared with 60 min in case of naked SPION. This additional time allows the nanocrystals to grow and accordingly surface coated SPION would be almost similar to the naked SPION in size.

3.3. Magnetization Properties. The superparamagnetic characterization of the nanoparticles was done using vibrating sample magnetometer (VSM), with a magnetic field in the range of –10000 to 10000 Oe, where parameters as saturation magnetization (Ms) and hysteresis loop were evaluated. Figure 3 shows the magnetization curve of the nanoparticles

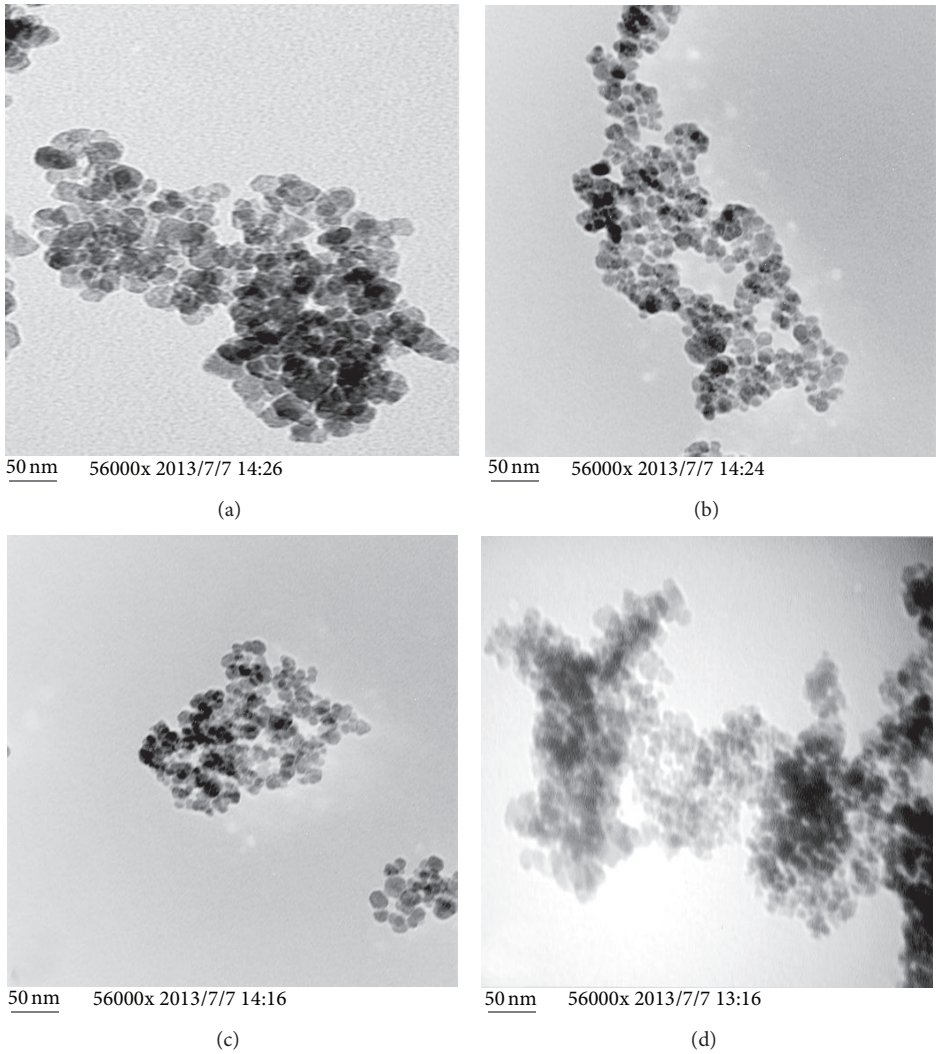

Figure 2: TEM micrographs of naked SPION (a) and surface modified SPION: L14@Fe_3O_4 (b), L4@Fe_3O_4 (c), and Gly@Fe_3O_4 (d).

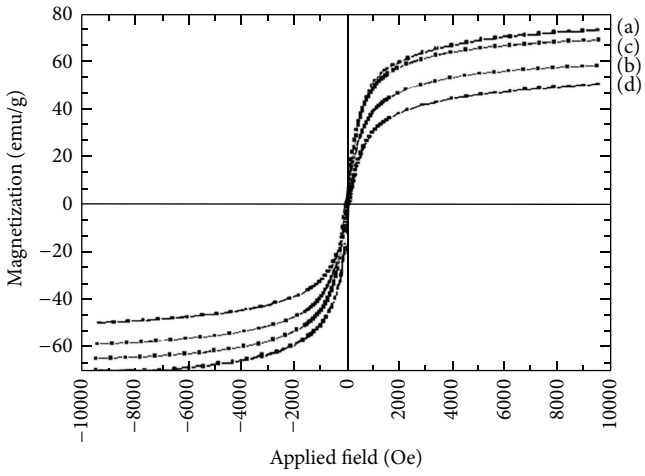

Figure 3: Magnetization curve of naked SPION (a) and surface modified SPION: L14@Fe_3O_4 (b), L4@Fe_3O_4 (c), and Gly@Fe_3O_4 (d) at room temperature.

at room temperature. All synthesized nanomagnets indicate a superparamagnetic behavior, as evidenced by negligible coercivity and remanence on the magnetization loop at 300 K. The Ms values of the naked SPION L14@Fe_3O_4, L4@Fe_3O_4, and Gly@Fe_3O_4 were found to be 73.0, 57.8, 71.18, and 50.1 emu/g, respectively. Due to diamagnetic properties of amino acid like materials, magnetic saturation of L14@Fe_3O_4, L4@Fe_3O_4, and Gly@Fe_3O_4 was reduced. It has been demonstrated that if the excess amount of amino acid (and probably lipoamino acid) was added to the synthesis reaction of magnetite nanoparticles and the intensity of coating was increased, saturation magnetization of resulting nanoparticles was decreased [26]. Nonetheless, this reduction due to amino and lipoamino acid coating is insignificant compared to naked SPION, while the reduction in magnetization by other biocompatible coatings such as polymeric and silica coating is considerably high [27]. Therefore, L14@Fe_3O_4, L4@Fe_3O_4, and Gly@Fe_3O_4 were still regarded as superparamagnetic particles.

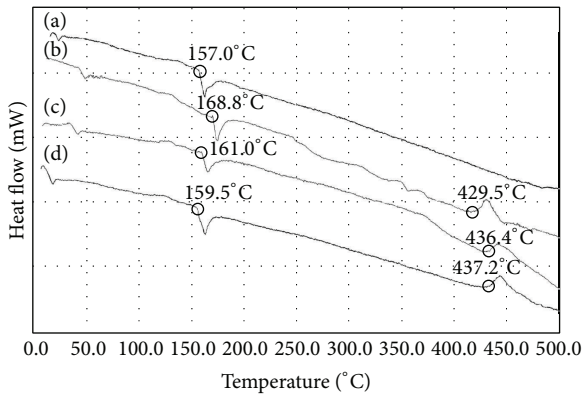

Figure 4: DSC diagrams of naked SPION (a) and surface modified SPION: L14@Fe_3O_4 (b), L4@Fe_3O_4 (c), and Gly@Fe_3O_4 (d).

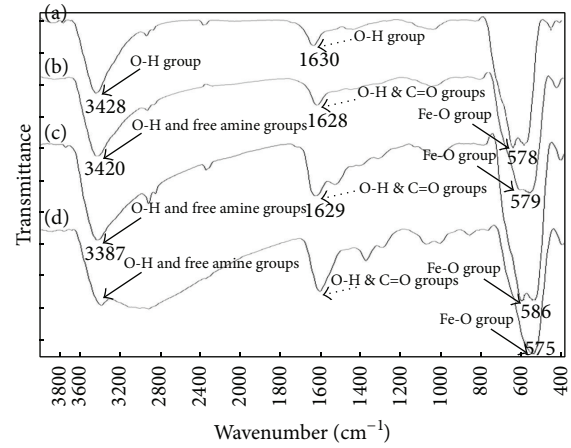

Figure 5: FT-IR analysis of naked SPION (a) and surface modified SPION: L14@Fe_3O_4 (b), L4@Fe_3O_4 (c), and Gly@Fe_3O_4 (d).

3.4. Thermal Analysis. DSC diagrams of naked and surface modified SPION over the range of 25°C to 499°C are indicated in Figure 4. As shown in the figure, for each nanoparticle, there was an endothermic peak between 150°C and 200°C that appeared because of oxidation and change in crystallinity of Fe_3O_4 [27]. These peaks appeared at 157°C in the curve of naked SPION and at 168.8°C, 161°C, and 159.5°C in the curves of L14@Fe_3O_4, L4@Fe_3O_4, and Gly@Fe_3O_4, respectively. The difference between temperatures which peaks occur in may because amino and lipoamino acid coated nanoparticles were oxidized at higher temperature. Previous studies show that magnetite crystal size influenced transformation from magnetite to maghemite by oxidation [27]. The smaller nanoparticles, which have been synthesized in the presence of L14@Fe_3O_4, are more stable and oxidized in higher temperatures. In curves (b), (c), and (d) of Figure 4, there was an exothermic peak at 429.5°C, 436.4°C, and 437.2°C, respectively, that appeared due to decomposition of amino and lipoamino acid on the surface of nanoparticles [28]. The temperature which this decomposition occurs in was dependent on type of coating.

3.5. FT-IR Analysis. FT-IR analysis of naked SPION and surface modified SPION was performed to characterize the surface nature of these particles and study the coating properties of the magnetite surface. As depicted in Figure 5, the presence of Fe_3O_4 in all studied nanoparticle can be confirmed by a strong absorption peak at around 570 cm^{-1}, which corresponds to the ν_1 band FeO structure of bulk magnetite [29]. Furthermore, an adsorption band was observed at around 400 cm^{-1}, which corresponds to the shifting of the ν_2 FeO band of bulk magnetite (at 375 cm^{-1}) to a higher wavenumber.

Also in Fe_3O_4 nanoparticles, due to covering of hydroxyl groups on the iron oxide surfaces, an intense and broad peak appeared in the 3200–3600 cm^{-1} region, corresponding to the OH stretching vibration [30]. In naked SPION, two peaks appeared around 1630 and 3400 cm^{-1} due to deforming and stretching of OH groups on the surface of magnetite nanoparticles. In L14@Fe_3O_4, L4@Fe_3O_4, and Gly@Fe_3O_4,

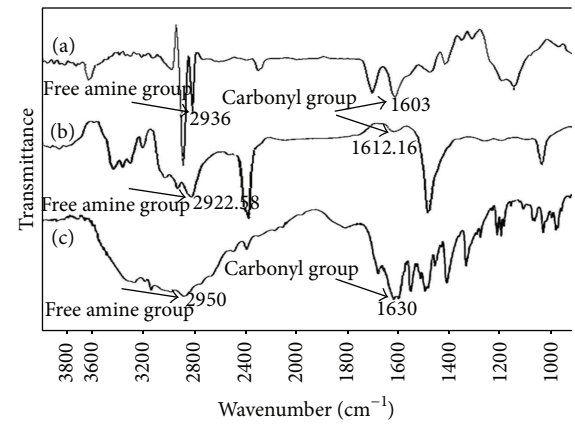

Figure 6: FTIR spectra of LAA14 (a), LAA4 (b), and pure glycine (c).

existence of a peak at 1630 cm^{-1} showed overlapping of OH deforming and CO stretching vibration of carboxylic groups. The amine and lipoamino acid groups are adsorbed on the magnetite surface by FeOC bonds. The two broad bands at around 1630 and 3400 cm^{-1} can be ascribed to the OH deforming vibration and NH stretching mode of NH_2 group, respectively. Furthermore, hydrogen bonds also have absorption around 3200. The presence of the anchored alkyl group was confirmed by CH stretching vibrations that appeared at 2900 cm^{-1} [30].

FTIR was further extended to study the pure glycine and lipoamino acids (Figure 6). FTIR spectra of pure glycine, LAA4, and LAA14 show peaks at 3000 and 1600 cm^{-1} due to free OH and CO stretching vibration of carboxylic acid groups and 3200 and 1550 cm^{-1} due to stretching and deforming vibration of amine NH, respectively.

3.6. Cytotoxicity and Morphology Studies. The MTT assay is a common and suitable method for evaluation of cell viability

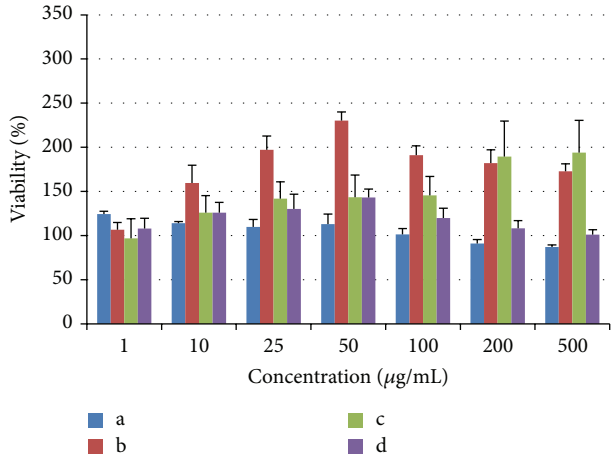

FIGURE 7: Cell viability of MTT assay results for all concentrations of uncoated SPION (a), L14@Fe_3O_4 (b), L4@Fe_3O_4 (c), and Gly@Fe_3O_4 (d) on Hep-G2 cells after 24 h in comparison with control (untreated cells) as 100%.

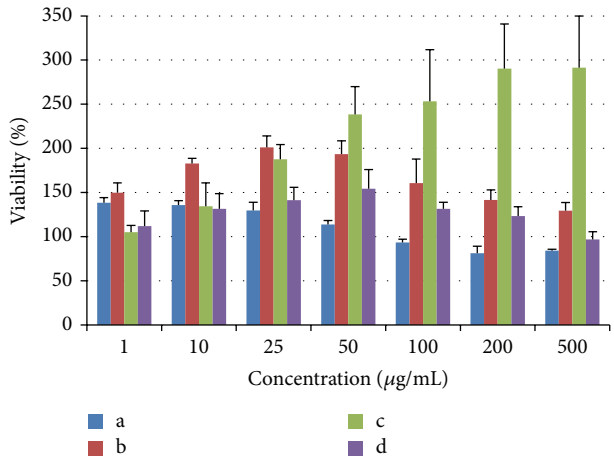

FIGURE 8: Cell viability of MTT assay results for all concentrations of uncoated SPION (a), L14@Fe_3O_4 (b), L4@Fe_3O_4 (c), and Gly@Fe_3O_4 (d) on Hep-G2 cells after 48 h in comparison with control (untreated cells) as 100%.

and detection of biomaterial toxicity [31]. This assay is based on mitochondrial activity and metabolism of cells.

In present assay, the proliferation/viability of hepatocarcinoma cells was determined after 24 (Figure 7) and after 48 h (Figure 8) treatment with nanoparticles. These results indicated that proliferation of cells was more desirable with surface modified SPION than naked ones. Metabolic activity was affected by all SPION in a dose and time dependent manner when nanoparticles were added in the concentration range of 1–500 μg/mL to wells containing the Hep-G2 cells. As observed in Figure 7, the cytotoxicity of the naked SPION increased in relation to increasing concentration. At a certain time (24 h, Figure 7), because of increasing concentration from 1 to 500 μg/mL, the viability percent was decreased from 124% to approximately 87%. On the other hand at certain concentration (200 μg/mL), the viability of cells at 24 and 48 h was 91% and 81%, respectively. When the cells were incubated with naked SPION with concentrations from 1 to 100 μg/mL within 24 and 48 hours, the cell viability was more than 100%. In contrast, at 200 μg/mL and higher concentrations, the Hep-G2 cells exhibited substantial loss in viability of about 20%. The improved viability of cells in low concentrations of SPION may be described by nutrient effect [32]. It is obvious that SPION are degraded and released iron ions in acidic lysosomal compartment [33]. These ions can be metabolized and used as a source of iron [8]. Such ionic iron is more beneficial for cancer cell line than normal ones because cancer cells have faster proliferation and thus require more ionic ions. Advanced cancer cells satisfy this requirement by overexpression of float receptors and transferrin protein on the cell membrane [34]. However, this effect is not improved by further increasing concentration of SPION. It was revealed that, in high concentrations, naked SPION can increase propensity to cross the tissue barriers and cellular membranes and, thereupon, increase cell tensions and potentially induce destruction of the main cellular components such as nucleus, nucleic acids, and mitochondria [35]. All these happenings are due to release of free ionic iron from the SPION that could catalyze production of reactive oxygen species (ROS) in Fenton's reaction [36]. The toxic effect of naked SPION and even some SPION with biocompatible coating on animal cells was previously reported by many toxicological researchers [31].

Comparing to the naked SPION, the results for the surface modified ones are to some extent different. They showed much less cytotoxicity on Hep-G2 and the cell viability remained more than 100% in comparison to control at a concentration as high as 1 μg/mL. The viability percent of cells was increased in a time-dependent manner as well as concentration-dependent behavior, when surface modified SPION were exposed to Hep-G2 cell lines for 24 and 48 hours. After 24 h, L14@Fe_3O_4 at concentrations from 1 to 50 μg/mL increased viability of the cells from 107 to 230% depending on the nanoparticle concentration in the medium. At higher concentrations (to 500 μg/mL), L4@Fe_3O_4 continues the same trend but viability of Hep-G2 cells in presence of L14@Fe_3O_4 and Gly@Fe_3O_4 at concentrations higher than 100 μg/mL was decreased. All these surface modified SPION continued in the same behavior after 48 h.

Variation in the shape and morphology of Hep-G2 cells can be visually evident upon their exposure to nanomaterials. Hence, the control and exposed cells were evaluated by optical microscopy to verify the toxicity or biocompatibility of the SPION. The results are shown in Figure 9 for control and L14@Fe_3O_4. Comparing to control group, the shape and general appearance of the cells exposed to surface modified SPION were not significantly affected. These cells had no significant physiological difference in contrast to control cells, when checked by optical microscopy.

The interaction between nanoparticles and eukaryotic cells is mainly related to surface properties of particle, which is governed by their chemistry, hydrophilic/hydrophobic characteristics, or surface energy. The adsorption of nanoparticles and their effect on cells was determined by these characteristics. Cell cytotoxicity assay showed that viability of the eukaryotic cells was found to be significantly reduced by

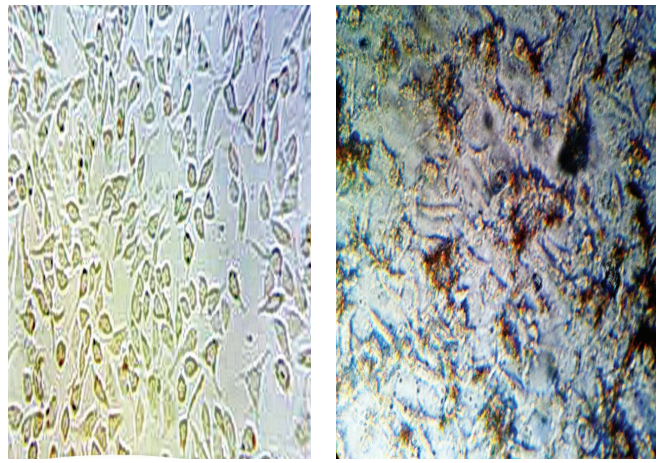

(a) (b)

Figure 9: Optical microscopy of untreated Hep-G2 cells (a) and Hep-G2 cells treated with 50 μg/mL L14@Fe_3O_4 (b).

naked magnetic nanoparticles compared to nonexposed cells. This might be due to large SPION take-up by the cells through endocytosis and consequently apoptosis promotion induced by free iron ions released from SPION. It is proved that ionic iron is a strong catalyzer of Fenton's reaction generating highly reactive radicals which cause cell membrane (lipid-protein) peroxidation and cell death [37]. Furthermore, cells growing in the presence of ionic iron form senile and disintegrated cellular debris [38]. Generally, L14@Fe_3O_4 and L4@Fe_3O_4 have the most biocompatibility among all tested magnetic nanoparticles. The noncytotoxic and viability promoting effect of nanoparticles coated with LAAs even at high concentrations can be attributed to the nature of LAAs. They are lipidic amino acids that play an efficient role in conjugation with a wide variety of therapeutic agents to increase their cellular internalization [39] and bioavailability. By selecting an appropriate side chain moiety for LAAs, they can deliver the conjugated drug to the specific organ [39, 40]. LAAs as part of drug delivery systems make hydrophilic agents as prodrugs that improve absorption and metabolic stability but the auxiliary groups are labile under biological conditions and the original drug is regenerated at some point on its journey to the site of action [40]. Accordingly, LAAs have been considered as parenteral drug carriers for sustained release and organ targeting [39, 41]. LAA coated SPION probably behave in the same way. The ionic iron may gradually be released from these nanoparticles and act as nutritional supplement. In fact in conjugation with LAA, the nutrient effect of SPION will be the dominant mechanism of action because free iron ion concentration in biological fluids is maintained in synergetic levels. The effect of LAA coated SPION is related to their concentration and the viability gradually decreases at concentration higher than 50 μg/mL. It seems that, in this condition, the toxic effects outweigh the beneficial effects and devolution in viability will appear. Also, this situation may be explained by SPION agglomeration and reduction in their effective concentration. SPION tend to adsorb protein compounds found in media as a result of surface net charges and ratio of large surface area to volume, so they consequently undergo agglomeration. In media like RPMI1640, the size of these agglomerates was reported about 10 times greater than the initial sizes. The composition of media and coating of nanoparticles have a substantial impact on the rate of agglomeration [24, 42].

LAAs at present are useful chemical substances for enhancing the absorption of poorly absorbed therapeutic agents and have been applied in targeted drug delivery of antibiotics [43], anti-inflammatory [40] and antitumor agents [41], alkaloids [41], CNS drugs, and peptides [44]. LAA consists of hydrophilic groups and a hydrophobic side chain. The strong attachment of the LAA molecules on the surface of a particle may lead to the steric stabilization of the compound, so that the particles escape from reticuloendothelial system (RES) uptake. Heretofore, a wide variety of SPION has been synthetized and used for numerous experimental, preclinical, and clinical purposes [31]. The blood half-life of naked SPION is pretty short and this problem limits its application in many cases. Surface modification is a common way to decrease the RES clearance and increase the circulation lifetime of iron oxide nanoparticles [45]. Therefore, this study suggested that LAA coated SPION are nontoxic and biocompatible nanoparticles for Hep-G2 cell line that can be alternatively used for diagnostic purposes such as perfusion, receptor and specific target imaging, imaging of lymph node, and vascular compartment (magnetic resonance angiography) and also may be applicable for therapeutic trials [12]. Further study about cytotoxicity of SPION coated with new LAAs with a different side chain and chemical moiety may lead to additional information about their biocompatibility and mechanism of action.

4. Conclusion

At the present study, we studied the cytotoxic effects of naked and some surface coated SPION on hepatocarcinoma cells

(Hep-G2). Our results revealed that SPION at lower concentrations can be beneficial for these cells because of their nutrient effect. However, at concentrations higher than 50 μg/mL the trend was reversed and the cell viability was decreased. Generally, it was concluded that SPION have dual impact on Hep-G2: cell growth promotion and toxicity. In the initial phase (at concentrations from 1 to 50 μg/mL), the dominant mechanism is the former one; however, by increasing nanoparticles concentration, cytotoxic effect progressively rises and eventually becomes the main mechanism, if aggregation or sedimentation of particles did not happen. Surface modification of SPION especially the ones coated with LAAs can maintain growth-enhancing effect. The reason may be the controlled release of ionic iron into the cells. Biocompatible LAA coated SPION can be used as targeted delivery of materials for diagnostic and therapeutic purposes.

Conflict of Interests

The authors declare that there is no conflict of interests regarding the publication of this paper.

Acknowledgments

This paper is based on the Ph.D. degree thesis of Ahmad Gholami. The authors thank the research council of Shiraz University of Medical Science for supporting this research (proposal submitted no. 30), Pharmaceutical Sciences Research Center, and Milad Mohkam for their valuable comments that improved the quality of the paper.

References

[1] K. W. Huang, S. Y. Yang, H. E. Horng et al., "Time-evolution contrast of target MRI using high-stability antibody functionalized magnetic nanoparticles: an animal model," *Journal of Nanomaterials*, vol. 2014, Article ID 351848, 7 pages, 2014.

[2] M. Ahamed, H. A. Alhadlaq, J. Alam, M. A. Majeed Khan, D. Ali, and S. Alarafi, "Iron oxide nanoparticle-induced oxidative stress and genotoxicity in human skin epithelial and lung epithelial cell lines," *Current Pharmaceutical Design*, vol. 19, no. 37, pp. 6681–6690, 2013.

[3] C. C. Berry, S. Wells, S. Charles, G. Aitchison, and A. S. G. Curtis, "Cell response to dextran-derivatised iron oxide nanoparticles post internalisation," *Biomaterials*, vol. 25, no. 23, pp. 5405–5413, 2004.

[4] A. K. Gupta and M. Gupta, "Synthesis and surface engineering of iron oxide nanoparticles for biomedical applications," *Biomaterials*, vol. 26, no. 18, pp. 3995–4021, 2005.

[5] M. M. Lin, H.-H. Kim, H. Kim, M. Muhammed, and D. K. Kim, "Iron oxide-based nanomagnets in nanomedicine: fabrication and applications," *Nano Reviews*, vol. 1, pp. 4883–4899, 2010.

[6] A. Singh and S. K. Sahoo, "Magnetic nanoparticles: a novel platform for cancer theranostics," *Drug Discovery Today*, vol. 19, no. 4, pp. 474–481, 2014.

[7] H.-W. Yang, M.-Y. Hua, H.-L. Liu, C.-Y. Huang, and K.-C. Wei, "Potential of magnetic nanoparticles for targeted drug delivery," *Nanotechnology, Science and Applications*, vol. 5, no. 1, pp. 73–86, 2012.

[8] N. Singh, G. J. Jenkins, R. Asadi, and S. H. Doak, "Potential toxicity of superparamagnetic iron oxide nanoparticles (SPION)," *Nano Reviews*, vol. 1, pp. 5358–5375, 2010.

[9] H. L. Karlsson, P. Cronholm, J. Gustafsson, and L. Möller, "Copper oxide nanoparticles are highly toxic: a comparison between metal oxide nanoparticles and carbon nanotubes," *Chemical Research in Toxicology*, vol. 21, no. 9, pp. 1726–1732, 2008.

[10] X. Wu, Y. Tan, H. Mao, and M. Zhang, "Toxic effects of iron oxide nanoparticles on human umbilical vein endothelial cells," *International Journal of Nanomedicine*, vol. 5, no. 1, pp. 385–399, 2010.

[11] M. Mahmoudi, A. Simchi, M. Imani et al., "A new approach for the *in vitro* identification of the cytotoxicity of superparamagnetic iron oxide nanoparticles," *Colloids and Surfaces B: Biointerfaces*, vol. 75, no. 1, pp. 300–309, 2010.

[12] A. K. Gupta and S. Wells, "Surface-modified superparamagnetic nanoparticles for drug delivery: preparation, characterization, and cytotoxicity studies," *IEEE Transactions on Nanobioscience*, vol. 3, no. 1, pp. 66–73, 2004.

[13] T. Lozano, M. Rey, E. Rojas et al., "Cytotoxicity effects of metal oxide nanoparticles in human tumor cell lines," *Journal of Physics: Conference Series*, vol. 304, no. 1, Article ID 012046, 2011.

[14] J.-S. Kim, T.-J. Yoon, K.-N. Yu et al., "Cellular uptake of magnetic nanoparticle is mediated through energy-dependent endocytosis in A549 cells," *Journal of Veterinary Science*, vol. 7, no. 4, pp. 321–326, 2006.

[15] Y. Ge, Y. Zhang, J. Xia et al., "Effect of surface charge and agglomerate degree of magnetic iron oxide nanoparticles on KB cellular uptake *in vitro*," *Colloids and Surfaces B: Biointerfaces*, vol. 73, no. 2, pp. 294–301, 2009.

[16] "Determining cytotoxicity of nano iron oxide in HepG2 cell line using MTT assay," in *Proceedings of the 6th International Symposium on Recent Advances in Environmental Health Research*, A. Patlolla, A. Berry, D. Land, and P. Tchounwou, Eds., Jackson, Miss, USA, 2009.

[17] A. Ebrahiminezhad, S. Rasoul-Amini, A. Kouhpayeh, S. Davaran, J. Barar, and Y. Ghasemi, "Impacts of amine functionalized iron oxide nanoparticles on HepG2 cell line," *Current Nanoscience*, vol. 10, no. 6, pp. 1–7, 2014.

[18] P. Clapés and M. R. Infante, "Amino acid-based surfactants: enzymatic synthesis, properties and potential applications," *Biocatalysis and Biotransformation*, vol. 20, no. 4, pp. 215–233, 2002.

[19] A. Wong and I. Toth, "Lipid, sugar and liposaccharide based delivery systems," *Current Medicinal Chemistry*, vol. 8, no. 9, pp. 1123–1136, 2001.

[20] R. Pignatello, A. Mangiafico, L. Basile, B. Ruozi, and P. M. Furneri, "Amphiphilic ion pairs of tobramycin with lipoamino acids," *European Journal of Medicinal Chemistry*, vol. 46, no. 5, pp. 1665–1671, 2011.

[21] W. A. Gibbons, R. A. Hughes, M. Charalambous et al., "Lipidic peptides, I. Synthesis, resolution and structural elucidation of lipidic amino acids and their homo- and hetero-oligomers," *Liebigs Annalen der Chemie*, vol. 1990, no. 12, pp. 1175–1183, 1990.

[22] S.-Y. Zhao, D. K. Lee, C. W. Kim, H. G. Cha, Y. H. Kim, and Y. S. Kang, "Synthesis of magnetic nanoparticles of Fe_3O_4 and $CoFe_2O_4$ and their surface modification by surfactant adsorption," *Bulletin of the Korean Chemical Society*, vol. 27, no. 2, pp. 237–242, 2006.

[23] F.-Y. Cheng, C.-H. Su, Y.-S. Yang et al., "Characterization of aqueous dispersions of Fe_3O_4 nanoparticles and their biomedical applications," *Biomaterials*, vol. 26, no. 7, pp. 729–738, 2005.

[24] H. L. Karlsson, J. Gustafsson, P. Cronholm, and L. Möller, "Size-dependent toxicity of metal oxide particles-A comparison between nano- and micrometer size," *Toxicology Letters*, vol. 188, no. 2, pp. 112–118, 2009.

[25] A. Ebrahiminezhad, S. Davaran, S. Rasoul-Amini, J. Barar, M. Moghadam, and Y. Ghasemi, "Synthesis, characterization and anti-listeria monocytogenes effect of amino acid coated magnetite nanoparticles," *Current Nanoscience*, vol. 8, no. 6, pp. 868–874, 2012.

[26] Z. Wang, H. Zhu, X. Wang, F. Yang, and X. Yang, "One-pot green synthesis of biocompatible arginine-stabilized magnetic nanoparticles," *Nanotechnology*, vol. 20, no. 46, Article ID 465606, 2009.

[27] A. Akbarzadeh, H. Mikaeili, N. Zarghami, R. Mohammad, A. Barkhordari, and S. Davaran, "Preparation and in vitro evaluation of doxorubicin-loaded Fe_3O_4 magnetic nanoparticles modified with biocompatible copolymers," *International Journal of Nanomedicine*, vol. 7, pp. 511–526, 2012.

[28] K. Can, M. Ozmen, and M. Ersoz, "Immobilization of albumin on aminosilane modified superparamagnetic magnetite nanoparticles and its characterization," *Colloids and Surfaces B: Biointerfaces*, vol. 71, no. 1, pp. 154–159, 2009.

[29] A. Ebrahiminezhad, Y. Ghasemi, S. Rasoul-Amini, J. Barar, and S. Davaran, "Preparation of novel magnetic fluorescent nanoparticles using amino acids," *Colloids and Surfaces B: Biointerfaces*, vol. 102, pp. 534–539, 2013.

[30] L. Zhang, B. Liu, and S. Dong, "Bifunctional nanostructure of magnetic core luminescent shell and its application as solid-state electrochemiluminescence sensor material," *Journal of Physical Chemistry B*, vol. 111, no. 35, pp. 10448–10452, 2007.

[31] H. Markides, M. Rotherham, and A. J. El Haj, "Biocompatibility and toxicity of magnetic nanoparticles in regenerative medicine," *Journal of Nanomaterials*, vol. 2012, Article ID 614094, 11 pages, 2012.

[32] D. Fischer, Y. Li, B. Ahlemeyer, J. Krieglstein, and T. Kissel, "In vitro cytotoxicity testing of polycations: influence of polymer structure on cell viability and hemolysis," *Biomaterials*, vol. 24, no. 7, pp. 1121–1131, 2003.

[33] A. K. Gupta and M. Gupta, "Cytotoxicity suppression and cellular uptake enhancement of surface modified magnetic nanoparticles," *Biomaterials*, vol. 26, no. 13, pp. 1565–1573, 2005.

[34] J. Tao, Y.-Q. Liu, Y. Li et al., "Hypoxia: dual effect on the expression of transferrin receptor in human melanoma A375 cell line," *Experimental Dermatology*, vol. 16, no. 11, pp. 899–904, 2007.

[35] A. Kasten, C. Grüttner, J. Kühn et al., "Comparative *In Vitro* study on magnetic iron oxide nanoparticles for MRI tracking of adipose tissue-derived progenitor cells," *PLoS ONE*, vol. 9, no. 9, Article ID e108055, 2014.

[36] K. Müller, J. N. Skepper, M. Posfai et al., "Effect of ultrasmall superparamagnetic iron oxide nanoparticles (Ferumoxtran-10) on human monocyte-macrophages *in vitro*," *Biomaterials*, vol. 28, no. 9, pp. 1629–1642, 2007.

[37] G. Huang, H. Chen, Y. Dong et al., "Superparamagnetic iron oxide nanoparticles: amplifying ROS stress to improve anticancer drug efficacy," *Theranostics*, vol. 3, no. 2, pp. 116–126, 2013.

[38] A. V. Singh, V. Vyas, E. Maontani et al., "Investigation of in vitro cytotoxicity of the redox state of ionic iron in neuroblastoma cells," *Journal of Neurosciences in Rural Practice*, vol. 3, no. 3, pp. 301–310, 2012.

[39] S. Bollam, P. Kandadi, S. S. Apte, and K. Veerabrahma, "Development of indinavir submicron lipid emulsions loaded with lipoamino acids-*in vivo* pharmacokinetics and brain-specific delivery," *AAPS PharmSciTech*, vol. 12, no. 1, pp. 422–430, 2011.

[40] J. Blanchfield and I. Toth, "Lipid, sugar and liposaccharide based delivery systems 2," *Current Medicinal Chemistry*, vol. 11, no. 17, pp. 2375–2382, 2004.

[41] R. Pignatello, D. Paolino, V. Panto et al., "Lipoamino acid prodrugs of paclitaxel: synthesis and cytotoxicity evaluation on human anaplastic thyroid carcinoma cells," *Current Cancer Drug Targets*, vol. 9, no. 2, pp. 202–213, 2009.

[42] A. Petri-Fink, B. Steitz, A. Finka, J. Salaklang, and H. Hofmann, "Effect of cell media on polymer coated superparamagnetic iron oxide nanoparticles (SPIONs): colloidal stability, cytotoxicity, and cellular uptake studies," *European Journal of Pharmaceutics and Biopharmaceutics*, vol. 68, no. 1, pp. 129–137, 2008.

[43] R. Pignatello, A. Mangiafico, B. Ruozi, G. Puglisi, and P. M. Furneri, "Amphiphilic erythromycin-lipoamino acid ion pairs: characterization and in vitro microbiological evaluation," *AAPS PharmSciTech*, vol. 12, no. 2, pp. 468–475, 2011.

[44] I. Toth, "A novel chemical approach to drug delivery: lipidic amino acid conjugates," *Journal of Drug Targeting*, vol. 2, no. 3, pp. 217–239, 1994.

[45] L. Liu, T. K. Hitchens, Q. Ye et al., "Decreased reticuloendothelial system clearance and increased blood half-life and immune cell labeling for nano- and micron-sized superparamagnetic iron-oxide particles upon pre-treatment with Intralipid," *Biochimica et Biophysica Acta—General Subjects*, vol. 1830, no. 6, pp. 3447–3453, 2013.